

## Design and synthesis of dihydroindazolo[5,4-*a*]pyrrolo[3,4-*c*]carbazole oximes as potent dual inhibitors of TIE-2 and VEGF-R2 receptor tyrosine kinases

Reddeppareddy Dandu,<sup>a,\*</sup> Allison L. Zulli,<sup>a</sup> Edward R. Bacon,<sup>a</sup> Ted Underiner,<sup>a</sup> Candy Robinson,<sup>b</sup> Hong Chang,<sup>b</sup> Sheila Miknyoczki,<sup>b</sup> Jennifer Grobelny,<sup>b</sup> Bruce A. Ruggeri,<sup>b</sup> Shi Yang,<sup>c</sup> Mark S. Albom,<sup>c</sup> Thelma S. Angeles,<sup>c</sup> Lisa D. Aimone<sup>c</sup> and Robert L. Hudkins<sup>a</sup>

<sup>a</sup>Department of Medicinal Chemistry, Cephalon, Inc., 145 Brandywine Parkway, West Chester, PA 19380, USA

<sup>b</sup>Oncology Research, Cephalon, Inc., 145 Brandywine Parkway, West Chester, PA 19380, USA

<sup>c</sup>Lead Discovery and Profiling, Cephalon, Inc., 145 Brandywine Parkway, West Chester, PA 19380, USA

Received 19 December 2007; revised 31 January 2008; accepted 1 February 2008

Available online 7 February 2008

**Abstract**—Fused dihydroindazolopyrrolocarbazole oximes have been identified as low nanomolar, potent dual TIE-2 and VEGF-R2 receptor tyrosine kinase inhibitors with excellent cellular potency. Development of the structure–activity relationships (SAR) led to identification of compounds **35** and **40** as potent, selective dual TIE-2/VEGF-R2 inhibitors with favorable pharmacokinetic properties. Compound **35** was orally active in tumor models with no observed toxicity.

© 2008 Elsevier Ltd. All rights reserved.

Antiangiogenic therapy—inhibition of the generation and growth of new blood vessels from the endothelium of an existing vascular, an essential process required to support solid tumor growth and metastasis—remains an area of focused drug discovery research.<sup>1</sup> Angiogenesis and vasculogenesis are dynamic and complex processes that are critical during early embryonic development as well as in a number of disease processes including cancer, diabetic retinopathy, rheumatoid arthritis, psoriasis, and age-related macular degeneration.<sup>2–7</sup> The exact mechanisms that regulate these processes have not been completely characterized, however, normal vasculature development is believed to be dependent on vascular endothelial growth factor (VEGF) and its receptor tyrosine kinases, mainly VEGF-R2 and the angiopoietins (Ang-1 and Ang-2) and their receptor tyrosine kinase, primarily TIE-2. VEGF and VEGF-Rs, principally VEGF-R2, play an important role by directing the differentiation of meso-

dermal cells into endothelial cells and the proliferation and migration of endothelial cells to form tubular cells.<sup>8–10</sup> The angiopoietins (Ang-1 and Ang-2) and their receptor tyrosine kinases mainly TIE-2 are believed to be involved in the later stages of modulating cell–cell and cell–matrix interactions required for vasculature remodeling and maturation.<sup>11,12</sup> Thus, optimal anti-angiogenic kinase therapy may require concurrently blocking both TIE-2 and VEGF-R2 receptor signaling to significantly inhibit tumor growth and metastasis.<sup>9,13</sup>

Dual TIE-2/VEGF-R2 receptor tyrosine kinase inhibitors have been reported by Pfizer (thiazole **1**<sup>14</sup> TIE-2/VEGF-R2 IC<sub>50</sub> = 18/11 nM), GlaxoSmithKline (furo[2,3-*d*]pyrimidine **2**<sup>15</sup> TIE-2/VEGF-R2 IC<sub>50</sub> = 2/3 nM), and Amgen (pyridinyl pyrimidine **3**<sup>16</sup> TIE-2/VEGF-R2 IC<sub>50</sub> = 4/4 nM) (Fig. 1).

Previously we reported on our first generation pan-VEGF-R anti-angiogenic clinical candidate **4** (CEP-7055)<sup>17</sup> that advanced into phase 1 clinical trials (Fig. 2). Our objective for a second generation compound superior to CEP-7055 (in terms of biochemical, pharmacokinetic (PK), pharmacodynamic, and anti-tumor efficacy profiles) was to build in TIE-2 activity

**Keywords:** VEGF-R2; TIE-2; Angiogenesis; Tyrosine kinase inhibitors.

\* Corresponding author. Tel.: +1 610 738 6577; fax: +1 610 344 0200; e-mail: [dreddy@cephalon.com](mailto:dreddy@cephalon.com)

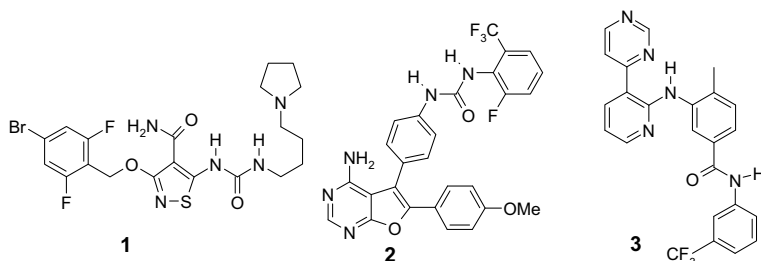


Figure 1. Structures of dual VEGF-R2/TIE-2 inhibitors.

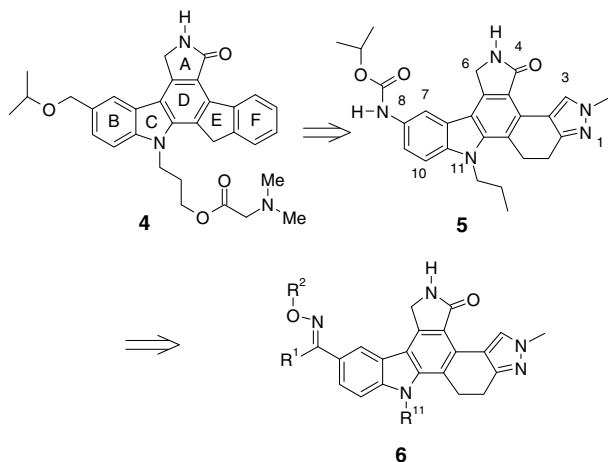
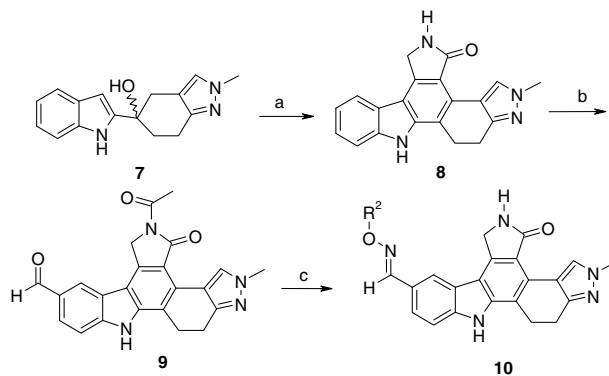


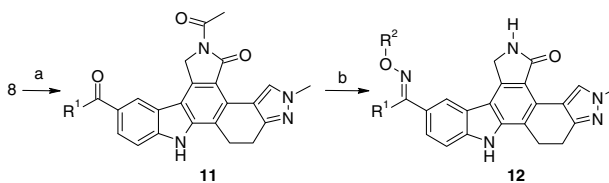
Figure 2. Design of dual VEGF-R2/TIE-2 inhibitors.

and improve upon the pharmacokinetic and in vivo profile of **4**. The project objective was to advance dual TIE-2/VEGF-R2 inhibitors with  $IC_{50}$  values less than 25 nM that demonstrated good cell potency and pharmacokinetic properties for in vivo evaluation. As a starting point to design in TIE-2 activity, structural modifications were made to the E- and F-rings ultimately identifying the N2-methyl dihydroindazole core (DHI) (see structure **8**; TIE-2  $IC_{50}$  = 1.3  $\mu$ M).<sup>18</sup> Early SAR development produced a series of carbamate (e.g., **5**) and urea dual TIE-2/VEGF-R2 inhibitors with good enzyme and cellular potency, but less than favorable pharmacokinetic properties. In addition, compound **5** displayed in vivo toxicity in tumor models.<sup>18</sup> In this paper we disclose the optimization and SAR for a series of C8 oxime dual inhibitors **6** with improved pharmacokinetic properties and significant oral in vivo anti-tumor efficacy.

The synthesis of DHI oximes **10**, **12**, and **16** commenced from common intermediate **7**.<sup>19</sup> Diels–Alder reaction of **7** with (Z)-3-cyanoacrylic acid ethyl ester, followed by DDQ oxidative aromatization and Raney-Ni reduction of the resulting cyano group led to lactam **8**<sup>20</sup> (Scheme 1). Lactam **8** was selectively protected with refluxing acetic anhydride to the N-acetyl, followed by a modified Duff reaction<sup>21</sup> with hexamethylenetetramine and trifluoroacetic acid to produce aldehyde **9**. Treatment of **9** with hydroxylamine hydrochloride or O-alkyl hydroxylamine hydrochloride, followed by hydrolysis of the N-acetyl with potassium carbonate in methanol produced the desired oximes **10**.



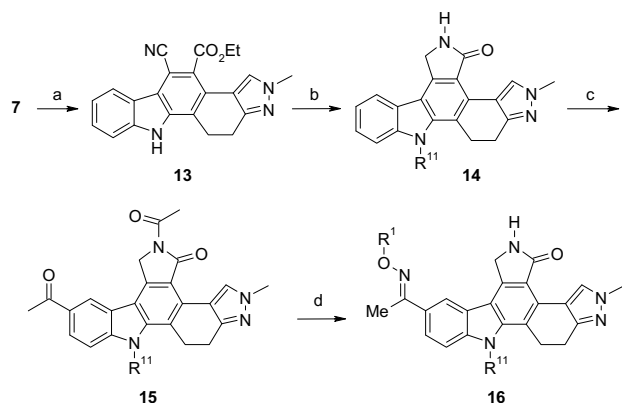
Scheme 1. Reagents and conditions: (a) i—(Z)-3-cyanoacrylic acid ethyl ester, YbBr<sub>3</sub>, 80 °C, AcOH; ii—DDQ, CH<sub>3</sub>CN; iii—Raney-Ni, DMF, MeOH, 50 psi, 27–30%; (b) i—Ac<sub>2</sub>O, reflux; ii—hexamethylenetetramine, TFA, reflux, 79–88%; (c) i—NH<sub>2</sub>OH·HCl or R<sup>2</sup>ONH<sub>2</sub>·HCl, NMP, EtOH, reflux; ii—K<sub>2</sub>CO<sub>3</sub>, MeOH, reflux, 50–55%.



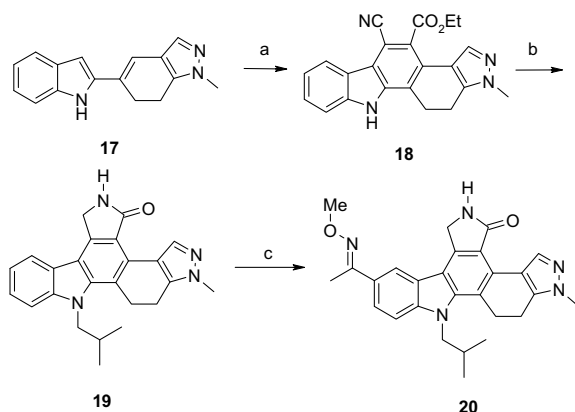
Scheme 2. Reagents and conditions: (a) i—acetyl chloride or isobutyryl chloride, AlCl<sub>3</sub>, CH<sub>2</sub>Cl<sub>2</sub>, MeNO<sub>2</sub>, rt; ii—Ac<sub>2</sub>O, reflux, 71–80%; (b) i—NH<sub>2</sub>OH·HCl or R<sup>2</sup>ONH<sub>2</sub>·HCl, NMP, EtOH, reflux; ii—K<sub>2</sub>CO<sub>3</sub>, MeOH, reflux, 65–72%.

Scheme 2 illustrates the synthesis of the second class of oximes **12**, prepared in an analogous manner to **10**. Friedel–Crafts acylation of **8** with acid chlorides and AlCl<sub>3</sub> followed by selective lactam N-acylation proceeded smoothly to **11**. Treatment of **11** with hydroxylamine hydrochloride or O-alkylhydroxylamines generated oximes **12** after deprotection.

The third class of N-alkyl oximes **16** is delineated in Scheme 3. Alkylation of the cyano-ester intermediate **13** (10 N NaOH, alkyl halide, acetone reflux) and reductive cyclization produced **14**.<sup>19</sup> Friedel–Crafts acylation of **14** followed by N-acetyl protection produced **15**. Oxime formation and removal of the acetyl group gave oximes **16**.



**Scheme 3.** Reagents and conditions: (a) *i*-(*Z*)-3-cyanoacrylic acid ethyl ester, YbBr<sub>3</sub>, 80 °C, AcOH; ii—DDQ, CH<sub>3</sub>CN, rt, 30–35%; (b) *i*—10 N NaOH, R<sup>11</sup>-I, acetone, reflux; ii—Raney-Ni, DMF, MeOH, 50 psi, 75–85%; (c) *i*—MeCOCl, AlCl<sub>3</sub>, CH<sub>2</sub>Cl<sub>2</sub>, CH<sub>3</sub>NO<sub>2</sub>, rt; ii—Ac<sub>2</sub>O, reflux, 50–55%; (d) *i*—NH<sub>2</sub>OH·HCl or R<sup>2</sup>ONH<sub>2</sub>·HCl, NMP, EtOH, reflux; ii—K<sub>2</sub>CO<sub>3</sub>, MeOH, reflux, 52–57%.



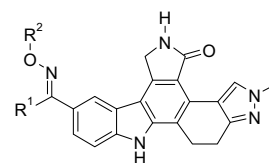
**Scheme 4.** Reagents and conditions: (a) *i*-(*Z*)-3-cyanoacrylic acid ethyl ester, YbBr<sub>3</sub>, 80 °C, AcOH; ii—DDQ, CH<sub>3</sub>CN, 30–35%; (b) *i*—10 N NaOH, 1-iodo-2-methylpropane, acetone, reflux; ii—Raney-Ni, DMF, MeOH, 50 psi, 82–85%; (c) *i*—MeCOCl, AlCl<sub>3</sub>, CH<sub>2</sub>Cl<sub>2</sub>, CH<sub>3</sub>NO<sub>2</sub>, rt; ii—MeONH<sub>2</sub>·HCl, Pyridine, 100 °C, 65–70%.

The N1 methyl pyrazole oxime **20** was prepared for comparison as described previously (Scheme 4) starting from the N1 methyl pyrazole diene **17**.<sup>19</sup>

The DHI oximes were screened against recombinant human VEGF-R2 and TIE-2 using a heterogeneous time-resolved fluorescence (TRF) readout and recombinant human phospholipase C-γ/glutathione *S*-transferase (GST) as substrate.<sup>17</sup> Shown in Table 1 are the structure–activity relationships (SAR) for the indole NH series (R<sup>11</sup> = H). The general SAR trend revealed the R<sup>2</sup> ether group was critical for TIE-2 potency, depending on R<sup>1</sup>. When R<sup>1</sup> = methyl, the optimum combination for dual potency was with R<sup>2</sup> = ethyl (**24**), *i*-propyl (**28**) or *i*-butyl (**29**). An alkyl group was preferred at R<sup>1</sup>, however increasing the size of the R<sup>1</sup> alkyl tended to decrease dual potency (compare **23**–**25**).

Compounds **24** (TIE-2 IC<sub>50</sub> = 23 nM, VEGF-R2 IC<sub>50</sub> = 2 nM), **28** (TIE-2 IC<sub>50</sub> = 28 nM, VEGF-R2

**Table 1.** SAR for R<sup>1</sup> and R<sup>2</sup>



Entry	R <sup>1</sup>	R <sup>2</sup>	TIE-2 <sup>a</sup>	VEGF-R2 <sup>a</sup>	VEGF-R2 <sup>22</sup> cell score
21	H	Me	148	18	ND
22	H	Et	264	4	ND
23	Me	Me	71	1	ND
24	Me	Et	23	2	4
25	<i>i</i> -Pr	Me	264	4	ND
26	<i>i</i> -Pr	Et	92	23	ND
27	Me	H	44	1	ND
28	Me	<i>i</i> -Pr	28	3	4
29	Me	<i>i</i> -Bu	10	10	4
30	Me	<i>t</i> -Bu	93	31	ND

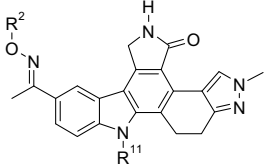
ND, not determined.

<sup>a</sup> IC<sub>50</sub> values in nM reported as the average of at least two separate determinations.

IC<sub>50</sub> = 3 nM) and **29** (TIE-2 IC<sub>50</sub> = 10 nM, VEGF-R2 IC<sub>50</sub> = 10 nM) had good dual enzyme potency and showed complete inhibition of VEGF-stimulated VEGF-R2 autophosphorylation in cells. However, in rat pharmacokinetic experiments they suffered from high clearance and short half-lives after iv administration. Therefore, attention shifted next to studying the R<sup>11</sup> indole position.

The SAR for R<sup>11</sup> alkyl substitutions are shown in Table 2. When R<sup>2</sup> = methyl, optimum dual potency was met with an R<sup>11</sup> 3-carbon chain (e.g., *n*-propyl **33** and *i*-butyl **35**). Unexpectedly, **33** (TIE-2 IC<sub>50</sub> = 30 nM and VEGF-R2 IC<sub>50</sub> = 1 nM) showed poor activity in the VEGF-R2 cell assay despite the potent VEGF-R2 enzyme activity. Compound **35** (TIE-2 IC<sub>50</sub> = 30 nM and VEGF-R2 IC<sub>50</sub> = 7 nM) showed complete inhibition of VEGF stimulated VEGF-R2 autophosphorylation in HUVECs.<sup>17</sup> Simultaneously increasing the R<sup>2</sup> and R<sup>11</sup> alkyl size decreased dual potency. From this set, the best combination for dual enzyme and cellular potency was met with R<sup>2</sup> = ethyl and R<sup>11</sup> = *i*-propyl (**40** TIE-2 IC<sub>50</sub> = 26 nM and VEGF-R2 IC<sub>50</sub> = 4 nM) or *i*-butyl (**37**, TIE-2 IC<sub>50</sub> = 30 nM and VEGF-R2 IC<sub>50</sub> = 1 nM). Further examination of the SAR around **40** by varying the R2 position (cf. **40**–**42**) demonstrated that increasing the size to *i*-butyl decreased VEGF-R2 and TIE-2 potency 13- and 2-fold, respectively. To evaluate the influence of the N2-methyl of **35** on dual potency, the N1-methyl regiomere **20** was synthesized and discovered it had 15- and 4-fold weaker activity for TIE-2 and VEGF-R2 (TIE-2 IC<sub>50</sub> = 461 nM and VEGF-R2 IC<sub>50</sub> = 28 nM) compared to **35**.

Based on their dual enzyme and cellular potency **35**, **37**, and **40** were evaluated for pharmacokinetic properties in the rat. Compounds **35** and **40** showed favorable PK in rat (Table 3), while **37** demonstrated poor oral bioavailability. The %*F* for **35** was estimated to be 66 after determining the plasma level exposure after iv (1 mg/kg) and

**Table 2.** SAR for R<sup>11</sup> and R<sup>2</sup>


Entry	R <sup>11</sup>	R <sup>2</sup>	TIE-2 <sup>a</sup>	VEGF-R2 <sup>a</sup>	VEGF-R2 <sup>22</sup> cell score
31	Me	Me	347	5	ND
32	Et	Me	300	4	ND
33	Pr	Me	30	1	1
34	<i>i</i> -Pr	Me	97	4	ND
35	<i>i</i> -Bu	Me	30	7	4
36	<i>n</i> -Bu	Me	108	12	ND
37	<i>i</i> -Bu	Et	25	4	4
38	<i>i</i> -Bu	<i>i</i> -Pr	52	31	4
39	<i>i</i> -Bu	<i>i</i> -Bu	23	94	ND
40	<i>i</i> -Pr	Et	26	4	4
41	<i>i</i> -Pr	<i>i</i> -Pr	66	11	4
42	<i>i</i> -Pr	<i>i</i> -Bu	46	51	2
43	Et	<i>i</i> -Bu	45	24	3

ND, not determined.

<sup>a</sup> IC<sub>50</sub> values in nM reported as the average of at least two separate determinations.**Table 3.** Rat pharmacokinetic properties for **35** and **40**

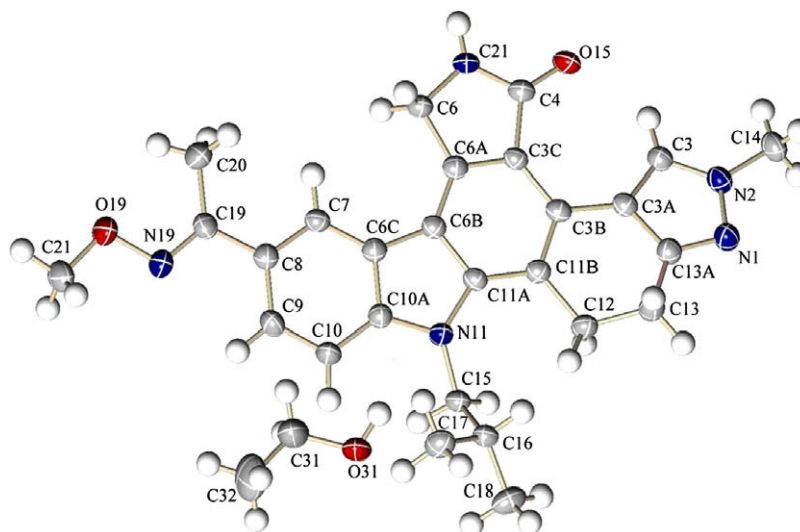
1 mg/kg iv	<b>35</b>	<b>40</b>	5 mg/kg po	<b>35</b>	<b>40</b>
<i>t</i> <sub>1/2</sub> (h)	1.4	2.0	% <i>F</i>	66	31
CL (mL/min/kg)	6.5	7.4	<i>t</i> <sub>1/2</sub> (h)	6.5	3.2
AUC <sub>0–∞</sub> (ng h/mL)	2762	2302	AUC <sub>0–∞</sub> (ng h/mL)	9055	3606
<i>V</i> <sub>d</sub> (L/kg)	0.8	1.3	<i>C</i> <sub>max</sub> (ng/mL)	874	637

po (5 mg/kg) administration over a 6-h period. The iv terminal half-life was 1.4 h with a volume of distribution of 0.8 L/kg and a clearance rate of 6.5 L/min/kg. The oral *C*<sub>max</sub> was 874 ng/mL (1.9 μM). Compound **40** also showed good oral exposure (%*F* = 31) and intrinsic pharmacokinetic properties (*t*<sub>1/2</sub> = 2 h, CL = 7.4 mL/min/kg) in the rat.

Homology modeling and docking experiments for VEGF-R2 were used to aid in developing and interpreting the dual SAR. For TIE-2, an X-ray co-crystal structure was solved with a DHI analog and subsequently, this structure was used for docking experiments with new analogs. Figure 4 shows **35** docked in the ATP pocket of the TIE-2 model. The lactam NH/CO form a bidentate donor/acceptor interaction with Glu903/Ala905 at the hinge region. The anti-oxime (=N) orientation serves as an acceptor for Asp982 backbone amide. The hydrophobic cavity that occupies the *O*-alkyl oxime is defined by Leu888, Leu976, Phe983, Gly984, Leu985 and Ile902. A single crystal structure<sup>23</sup> for **35** (Fig. 3) was solved that confirmed the *trans*-oxime orientation and the regiochemistry of the lactam carbonyl and the indazole N2 methyl group.

Compounds **35** and **40** were profiled for selectivity against a panel of tyrosine and serine/threonine kinases. Both compounds potently inhibited PDGFRβ (92% inhibition at 1 μM) and c-src (IC<sub>50</sub> = 43 nM and 14 nM for compounds **35** and **40**, respectively), but not EGFR or IR (IC<sub>50</sub> values >1 μM). Inhibition of the src family was also demonstrated for lyn, lck, fyn, yes and blk (>80% inhibition at 1 μM). In contrast, selectivity against a number of serine/threonine kinases was observed with weak inhibition for CDKs, CHK1, GSK 3β, JNKs, MAPK, MEK1 and the PKC isoforms. Compound **35** was found to potently inhibit VEGF-R1 and VEGF-R3 family members with IC<sub>50</sub> values of 8 and 10 nM, respectively.

Based on its dual in vitro activity, selectivity and PK properties, **35** was evaluated in both functional (ex vivo rat aortic ring explant cultures) and target-directed (in vitro HUVEC capillary-tube formation) bioassays in order to assess the anti-angiogenic activity and potential cytotoxic profile. Compound **35** displayed significant concentration-related inhibition of complete HUVEC capillary tube formation relative to control in the absence of apparent HUVEC cyto-

**Figure 3.** ORTEP drawing of the crystal structure of **35**.



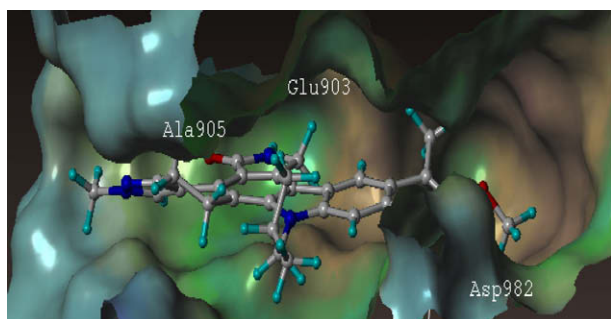


**Figure 4.** Hydrophobic surface map around compound **35** bound to the ATP site of TIE-2.

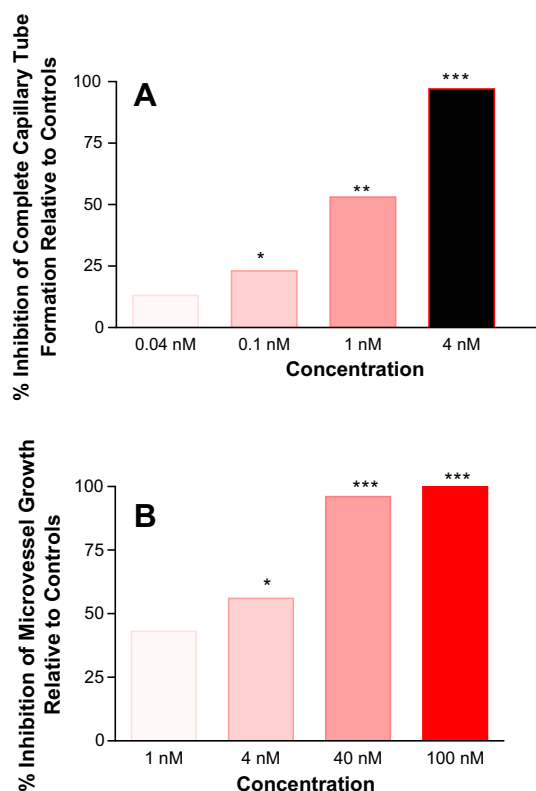


**Figure 5.** Anti-angiogenic activity of **35** in (A) VEGF-induced HUVEC capillary-tube formation and (B) ex vivo rat aortic ring explants.  $p < 0.05$ , \*\* $p < 0.01$ , \*\*\* $p < 0.0001$ .

toxicity (based upon blue exclusion) with an  $EC_{50}$  values of  $1 \pm 0.2$  nM. Complete inhibition of VEGF-induced HUVEC capillary-tube formation was achieved at concentrations greater than 4 nM (Fig. 5A).<sup>24</sup> The anti-angiogenic response to **35** was further evaluated ex vivo in rat aortic ring explants over a 10-day time course in the absence of exogenous VEGF stimulation. Concentration-related inhibitory effects on the peak phase of microvessel growth were observed with an  $EC_{50}$  of  $3.0 \pm 0.7$  nM (Fig. 5B). Complete inhibition of microvessel outgrowth was observed at concentrations greater than 50 nM. The anti-angiogenic effects of **35** in this assay were achieved in the absence of apparent cytotoxicity to endothelial cells, fibroblasts, and pericytes in primary aortic ring explant cultures.<sup>24</sup> The  $EC_{50}$  for inhibition of prolifer-

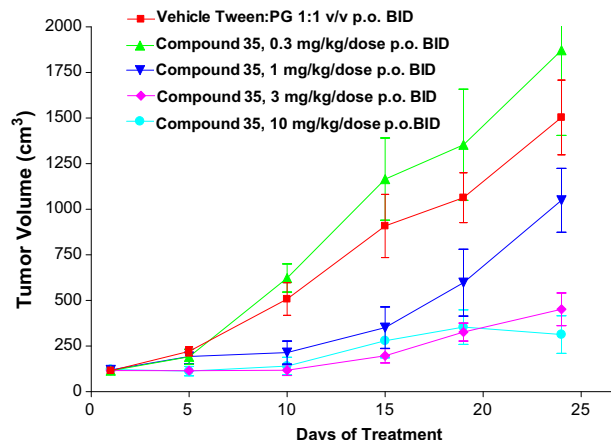


**Figure 6.** Effects of oral administration of compound **35** on human melanoma xenografts.

ation of five human tumor cell lines in vitro by **35** ranged from approximately 50 nM to greater than 1  $\mu$ M. Compound **35** had an  $EC_{50}$  of approximately 70 nM against A375 cells in vitro.

Based upon the demonstrated tolerability and anti-tumor and anti-angiogenic efficacy of **35** in the 10-day SVR angiosarcoma screening model, **35** was evaluated following chronic oral administration from 0.3 to 10 mg/kg/dose range in the A375 human tumor xenograft melanoma model for anti-tumor efficacy and tolerability (Fig. 6).<sup>23</sup> Chronic oral administration of **35** was well tolerated with no overt mortality or significant body weight loss. Compound **35** demonstrated significant, dose-related tumor growth inhibition and increase in the incidence of partial and complete regressions. At 10 mg/kg bid, a 38% incidence of partial tumor regressions and 80% inhibition of tumor growth relative to vehicle-treated control mice were observed. Complete tumor regressions were observed at 3 mg/kg bid as well.

In conclusion, we described here the in vitro optimization of a series of potent dual TIE-2/VEGF-R2 DHI-oximes with good pharmacokinetic properties. Compound **35** demonstrated potent dual enzyme and cellular activity, excellent rat pharmacokinetic properties and in vitro and oral in vivo anti-angiogenic activity consistent with the mechanism. Details of the in vitro and the in vivo results for **35** and **40** will be published in due course.

### Acknowledgments

The authors thank Drs. John P. Mallamo and Jeffry L. Vaught for support and helpful scientific discussions.

### References and notes

- Folkman, J.; Shing, Y. *J. Biol. Chem.* **1992**, *267*, 10931.
- (a) Carmeliet, P.; Jain, R. K. *Nature* **2000**, *407*, 249; (b) Folkman, J. *Nat. Med.* **1995**, *1*, 27.

3. Adamis, A. P.; Shima, D. T.; Yeo, K. T.; Yeo, T. K.; Brown, L. F.; Berse, B.; D'Amore, P. A.; Folkman, J. *J. Biochem. Biophys. Res. Commun.* **1993**, *193*, 631.
4. Giatromanolaki, A.; Sivridis, E.; Athanassou, N.; Zois, E.; Thorpe, P. E.; Brekken, R. A.; Gatter, K. C.; Harris, A. L.; Koukourakis, I. M.; Koukourakis, M. I. *J. Pathol.* **2001**, *194*, 101.
5. Detmar, M. *Dermatol. Sci.* **2000**, *24*, S78.
6. Folkman, J.; Klagsburn, M. *Science* **1987**, *235*, 442.
7. Folkman, J. *J. Natl. Cancer Inst.* **1991**, *82*, 4.
8. Ferrera, N.; Davis-Smyth, T. *Endocrine Rev.* **1997**, *18*, 4.
9. Borgstrom, P.; Hillman, K. J.; Sriramarao, P.; Ferrera, N. *Cancer Res.* **1996**, *56*, 4032.
10. Adamis, A. P.; Miller, J. W. *Arch. Ophthalmol.* **1996**, *114*, 66.
11. Koblizek, T. I.; Weiss, C.; Yancopoulos, G. D.; Deutsch, U.; Risau, W. *Curr. Biol.* **1998**, *8*, 529.
12. Witzenbichler, B.; Maisonpierre, P. C.; Jones, P.; Yancopoulos, G. D.; Isner, J. M. *J. Biol. Chem.* **1998**, *273*, 18514.
13. Lin, P.; Buxton, J. A.; Acheson, A.; Radziejewski, C.; Maisonpierre, P. C.; Yancopoulos, G. D.; Channon, K. M.; Hale, L. P.; Dewhirst, M. W.; George, S. E.; Peters, K. G. *Proc. Natl. Acad. Sci. U.S.A.* **1998**, *95*, 8829.
14. Beebe, J. S.; Jani, J. P.; Knauth, E.; Goodwin, P.; Higdon, C.; Rossi, A. M.; Emerson, E.; Finkelstein, M.; Floyd, E.; Harriman, S.; Atherton, J.; Hillerman, S.; Soderstrom, C.; Kou, K.; Gant, T.; Noe, M. C.; Foster, B.; Rastinejad, F.; Marx, M. A.; Schaeffer, T.; Whalen, P. M.; Roberts, W. G. *Cancer Res.* **2003**, *63*, 7301.
15. Miyazaki, Y.; Matsunaga, S.; Tang, J.; Maeda, Y.; Naano, M.; Philippe, R. J.; Shibahara, M.; Liu, W.; Sato, H.; Wang, L.; Nolte, R. T. *Bioorg. Med. Chem. Lett.* **2005**, *15*, 2203.
16. (a) Hodous, B. L.; Geuns-Meyer, S. D.; Hughes, P. E.; Albrecht, B. K.; Bellon, S.; Caenepeel, S.; Cee, V. J.; Chaffee, S. C.; Emery, M.; Fretland, J.; Gallant, P.; Gu, Y.; Johnson, R. E.; Kim, J. L.; Long, A. M.; Morrison, M.; Olivieri, P. R.; Patel, V. F.; Polverino, A. R.; Rose, P.; Wang, L.; Zhao, H. *Bioorg. Med. Chem. Lett.* **2007**, *17*, 2886; (b) Cee, V. J.; Albrecht, B. K.; Geuns-Meyer, S. D.; Hughes, P. E.; Bellon, S.; Bready, J.; Caenepeel, S.; Chaffee, S. C.; Coxon, A.; Emery, M.; Fretland, J.; Gallant, P.; Gu, Y.; Hodous, B. L.; Hoffman, D.; Johnson, R. E.; Kendall, R.; Kim, J. L.; Long, A. M.; McGowan, D.; Morrison, M.; Olivieri, P. R.; Patel, V. F.; Polverino, A.; Powers, P.; Rose, P.; Wang, L.; Zhao, H. *J. Med. Chem.* **2007**, *50*, 627; (c) Hodous, B. L.; Geuns-Meyer, S. D.; Hughes, P. E.; Albrecht, B. K.; Bellon, S.; Bready, J.; Caenepeel, S.; Cee, V. J.; Chaffee, S. C.; Coxon, A.; Emery, M.; Fretland, J.; Gallant, P.; Gu, Y.; Hoffman, D.; Johnson, R. E.; Kendall, R.; Kim, J. L.; Long, A. M.; Morrison, M.; Polverino, A. R.; Patel, V. F.; Polverino, A. R.; Rose, P.; Tempest, P.; Wang, L.; Whittington, D. A.; Zhao, H. *J. Med. Chem.* **2007**, *50*, 611.
17. Gingrich, D. E.; Reddy, D. R.; Iqbal, M. A.; Singh, J.; Aimone, L. D.; Angeles, T. S.; Albom, M.; Yang, S.; Ator, M. A.; Meyer, S. L.; Robinson, C.; Ruggeri, B. A.; Dionne, C. A.; Vaught, J. L.; Mallamo, J. P.; Hudkins, R. L. *J. Med. Chem.* **2003**, *46*, 5375.
18. Becknell, N. C.; Zulli, A. L.; Angeles, T. S.; Yang, S.; Albom, M. S.; Aimone, L. D.; Robinson, C.; Chang, H.; Hudkins, R. L. *Bioorg. Med. Chem. Lett.* **2006**, *16*, 5368.
19. (a) Josef, K. A.; Reddy, D. R.; Tao, M.; Hudkins, R. L. *J. Heterocycl. Chem.* **2006**, *43*, 719; (b) Reddy, D. R.; Tao, M.; Josef, K. A.; Bacon, E. R.; Hudkins, R. L. *J. Heterocycl. Chem.* **2007**, *44*, 437.
20. (a) Hudkins, R. L.; Zulli, A. L.; Reddy, D. R.; Gingrich, D. E.; Tao, M.; Becknell, N. C.; Diebold, J. L.; Underiner, T. L. PCT Application, W.O. Patent 05,063,763; (b) Hudkins, R. L.; Park, C. H. *J. Heterocycl. Chem.* **2003**, *40*, 135; (c) Hudkins, R. L.; Knight, Jr., E., U.S. Patent 5,705,511, 1997.
21. Plug, J. P. M.; Koomen, G.-J.; Pandit, U. K. *Synthesis* **1992**, 1221.
22. The data were scored based on decrease in protein band density at 50 nM compound concentration compared to VEGF-stimulated control (no inhibitor) as follows: 0 = no decrease; 1 = 1–25%; 2 = 26–50%; 3 = 51–75%; 4 = 76–100%.
23. The coordinates are available from the Cambridge Crystallographic Data Center (CCDC) and the reference number, CCDC 675560.
24. The complete details of the in vitro and the in vivo results for compounds **35** and **40** will be published elsewhere in due course.